

Imperfect Oriented Attachment: Dislocation Generation in Defect-Free Nanocrystals

R. Lee Penn and Jillian F. Banfield*

Dislocations are common defects in solids, yet all crystals begin as dislocation-free nuclei. The mechanisms by which dislocations form during early growth are poorly understood. When nanocrystalline materials grow by oriented attachment at crystallographically specific surfaces and there is a small misorientation at the interface, dislocations result. Spiral growth at two or more closely spaced screw dislocations provides a mechanism for generating complex polytypic and polymorphic structures. These results are of fundamental importance to understanding crystal growth.

Dislocations (line defects) are important features in crystals. Spiral growth, which occurs at sites where screw dislocations exit surfaces, can dominate growth kinetics (1), especially in cases where the driving force for crystal growth is low (2). Dislocations increase plasticity by several orders of magnitude (3), provide critical sites for nucleation during unmixing or phase transformations, are reactive sites in mineral dissolution, and greatly affect diffusion. However, nanocrystals are typically defect-free (4), and the origin of dislocations is often unclear (5). Here we present a mechanism for dislocation formation that may operate during early growth that involves attachment between two or more nanoparticles.

Recently we showed that when aggregates of nanocrystalline titania particles coarsen under hydrothermal conditions, oriented attachment becomes an important growth mechanism (6). Oriented attachment involves spontaneous self-organization of adjacent particles so that they share a common crystallographic orientation, followed by joining of these particles at a planar interface. Bonding between the particles reduces overall energy by removing surface energy associated with unsatisfied bonds (through complete elimination of the mineral-air or mineral-fluid interface). This mechanism is relevant in cases where particles are free to move (such as in solution or where particles have abundant surface-bound water) and probably occurs in nature (7). It may also apply when particles nucleate side-by-side on a substrate and coalesce during growth.

R. L. Penn, Materials Science Program, University of Wisconsin-Madison, Madison, WI 53706, USA. J. F. Banfield, Mineralogical Institute, Graduate School of Science, University of Tokyo, Hongo, Bunkyo-ku, Tokyo 113, Japan. E-mail: jill@min.su-tokyo.ac.jp

*To whom correspondence should be addressed. Permanent address: Department of Geology and Geophysics, University of Wisconsin-Madison, Madison, WI 53706, USA.

Oriented attachment can give rise to homogeneous single crystals or to crystals separated by twin boundaries or other planar defects (6, 8). Twins are formed when coherence is achieved in the plane of the interface, but the crystallographic axes in the material on opposite sides of the interface are related by a symmetry operation not found in the untwinned crystal (6, 8, 9). The atomic arrangement of the material composing the twin boundary may be distinct from the bulk and be structurally similar to a polymorph (10). In this case, the phase transformation product can nucleate preferentially within the twin slab. This process has been demonstrated for reactions relating anatase to brookite and anatase to rutile (8, 11), and may contribute to the size dependence of the transformation rate in nanocrystalline materials (11, 12).

In this report, we show that particle growth can involve attachment characterized by a small misorientation in the interface. We refer to this as imperfect oriented attachment. Imperfect oriented attachment of nanocrystals can generate dislocations with edge, screw, and mixed character. Because initial nanocrystals were defect free (4), any defects observed by high-resolution transmission electron microscopy (HRTEM) can be attributed to the growth process. Imperfect oriented attachment involving multiple particles may result in closely spaced dislocations with a wide range of Burgers vectors, possibly leading to the growth of complex long-period structures whose origin has remained obscure.

This study used nanocrystalline anatase (TiO_2) synthesized by the sol gel route (12). Impurities were removed by dialysis (6). The initial particles had a tight size distribution and diameters, measured by x-ray diffraction peak broadening analysis and HRTEM, of 5 to 6 nm (6, 12). These starting materials were coarsened in solution at 250°C and 40 bars in hydrothermal bombs (8). Reacted materials were characterized with a 200-kV HRTEM

with a spherical aberration constant of 0.5 mm. Particle morphology evolved rapidly, leading to crystals primarily bounded by low-energy {101} surfaces. Attachment typically occurs on high-surface-energy planes such as {112} or {001}.

An HRTEM image of a group of three attached particles with very similar orientations is shown in Fig. 1. Lattice fringe details indicate that the interface (arrows) between the top two particles involves rotation of one crystal relative to the other about an axis contained in the plane of the boundary (and normal to the page). The result is a series of edge dislocations (defined as having a Burgers vector normal to the dislocation line) similar to those seen in low-angle tilt boundaries.

The formation of dislocations at attachment interfaces is readily explained. When structurally similar surfaces of particles approach, there will be a driving force to form chemical bonds between atoms of opposing surfaces so as to achieve full coordination. However, typically, surfaces are not atomically flat. Coherence will then be achieved by distortion in some areas of the interface, and

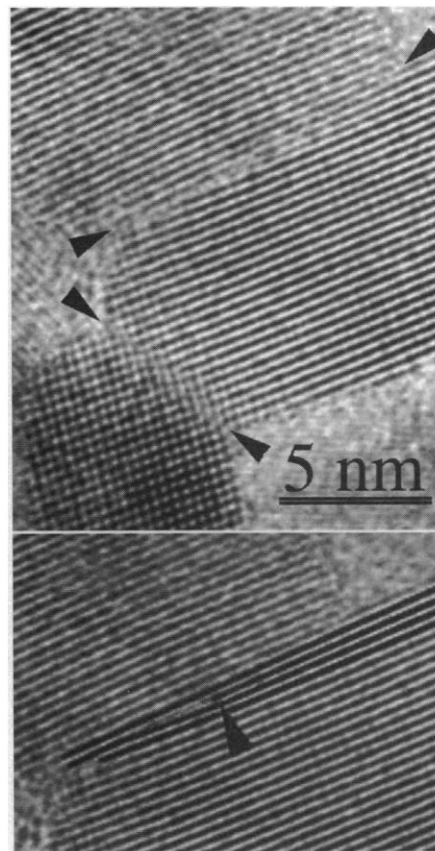


Fig. 1. HRTEM image of three attached TiO_2 particles. Arrowheads mark interfaces between primary particles. The edge dislocation at the upper interface is reproduced below, with lattice fringes around the terminating plane (arrowhead) highlighted for clarity.

REPORTS

edge dislocations will form in the regions of step sites (Fig. 2). Such imperfect oriented attachment can produce a range of dislocation types, from pure edge to pure screw, depending on the rotational relation of the primary crystallites. Screw dislocations will be formed when the axis of rotation is perpendicular to the plane of the interface (Burgers vector parallel to the dislocation line), and edge dislocations are formed when the axis of rotation is contained within the plane of the interface.

Imperfect attachment involving simple rotation of two particles about an axis normal to the interface has not been observed. A substantial driving force for crystal rotation to achieve full coherence is generally expected, but some rotations may be metastable and preserved by formation of a coincident site array. Regardless of whether boundaries bearing screw dislocations form by attachment involving two particles, they are predicted (Fig. 2) and observed (Fig. 3) where a third particle attaches across a low-angle tilt boundary.

The formation of screw dislocations when a third particle (top) attaches across a low-angle tilt boundary is schematically illustrated in Fig. 2. Although perfect coherence is achieved between the left-hand particle and the incoming third particle, the interface be-

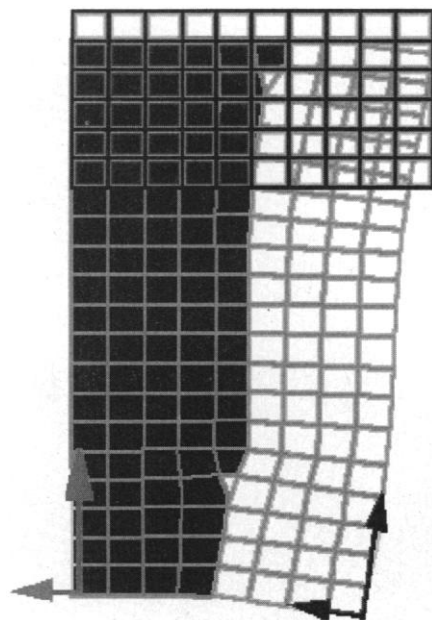


Fig. 2. Diagram illustrating the three particles. Initially, the two lower particles join, but a small rotation is introduced by surface steps on the particle to the left. A third particle (top) is attached in an oriented way to the crystal on the left, but a rotational misorientation occurs between it and the lower particle on the right. This idealized case illustrates the formation of edge dislocations (dislocation line normal to the page) and screw dislocations (dislocation line horizontal).

tween the right-hand particle and the third particle involves rotation. Elastic distortion will result in coherence over some regions and in the formation of screw dislocations. When attachment across a tilt boundary involves atomically rough surfaces such as steps, dislocations of mixed character will result.

An image of a crystal formed by attachment of at least four primary anatase crystallites is shown in Fig. 3. Small misorientations accompany edge defects (indicated by lines and arrows). Attachment of a particle (lower left) onto the aggregate containing edge defects (the crystal labeled 4) results in dislocations with screw character.

Recent molecular dynamical simulations predicted the formation of dislocations during sintering of nanocrystalline copper under high shear stress and also predicted the rotation of contacting particles (13). The prediction of rotation is important because it confirms the very strong driving force for particle orientation. These forces are expected to operate over a wide range of natural and experimental conditions.

Once dislocations with appreciable screw character are formed by oriented attachment, spiral growth may become the dominant growth mechanism. If the component of the Burgers vector normal to the surface is not an integral of the height of the unit cell repeat, a new polytype may develop, as has been suggested previously (14). Where two (or more) screw dislocations produced through imperfect oriented attachment are sufficiently closely spaced, growth initiated at both spirals may proceed simultaneously [as proposed for interlaced dislocation growth (15)]. Interlaced dislocation growth requires that screw dislocations be separated by less than π times the critical nucleus diameter (15). Thus, the necessary spacing

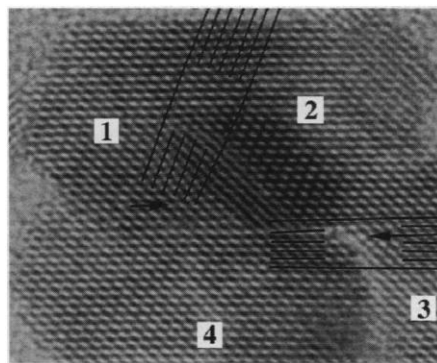


Fig. 3. HRTEM image (recorded down [100] anatase) of a portion of a crystal formed by attachment of at least four primary particles. Arrowheads and lines (spaced 0.48 nm apart) indicate four edge dislocations (best seen if viewed at a low angle). The left and right sides of particle 4, which rests on the other crystals, are apparent.

closely matches the spacing resulting from oriented attachment. If units to either side of an interface are related by twinning, the result of interlaced dislocation growth will be a new structure with the interstratification repeat equal to the sum of the Burgers vectors. A suite of long-period polytypes may result from interlayering of slabs of different thicknesses (due to combinations of different Burgers vectors).

Oriented attachment is not constrained to occur between crystals of a single structure [for example, it was shown to occur between two polymorphs of titania (8)] or composition. The only requirement is that the surfaces of the attaching particles be dimensionally similar. Where attachment involves two compounds that differ compositionally, structurally, or both, the result may be a long-period regular interstratification. As for polytypes, two screw dislocations will add to form one screw dislocation of $b_a + b_b$, resulting in interlayering of two structural units (Fig. 4). Spiral growth about multiple screw dislocations may provide a mechanism for the crystallization of regularly interstratified compounds belonging to polysomatic series (16). Because the magnitudes of the Burgers vector in each slab may differ significantly, an almost unlimited range of intergrowths is possible.

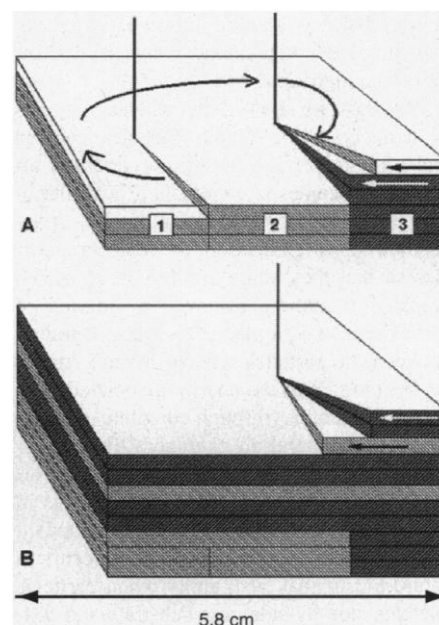


Fig. 4. Block diagrams illustrating simultaneous growth at two adjacent screw dislocations formed by imperfect oriented attachment involving three crystals (labeled 1, 2, and 3). Two crystals that differ in composition or orientation or both are joined at the right-hand interface. The screw to the left sweeps around, growing over the step that is two unit cells high at the right-hand interface (A). The result is a regular interstratification of the two materials (B).

References and Notes

1. The two most commonly noted mechanisms of crystal growth are spiral growth around a dislocation and surface nucleation followed by two-dimensional growth. Both mechanisms involve the addition of atoms to reactive surface sites from solution, vapor, or melt. W. K. Burton, N. Cabrera, F. C. Frank, *Nature* **163**, 398 (1949); L. J. Griffin, *Philos. Mag.* **41**, 196 (1950); W. K. Burton, N. Cabrera, F. C. Frank, *Philos. Trans. R. Soc. London A* **243**, 299 (1951); J. Friedel, *Dislocations* (Pergamon, New York, 1964). M. F. Hochella, *Mineral-Water Interface Geochemistry*, vol. 23 of *Reviews in Mineralogy*, M. F. Hochella and A. F. White, Eds. (Mineralogical Society of America, Washington, DC, 1990), pp. 87–132.
2. R. J. Kirkpatrick, *Kinetics of Geochemical Processes*, vol. 8 of *Reviews in Mineralogy*, A. S. Lasaga and R. J. Kirkpatrick Eds. (Mineralogical Society of America, Washington, DC, 1981), pp. 321–398.
3. A. Lasaga, *Kinetics of Geochemical Processes*, vol. 8 of *Reviews in Mineralogy*, A. S. Lasaga and R. J. Kirkpatrick Eds. (Mineralogical Society of America, Washington, DC, 1981), pp. 261–320.
4. A. P. Alivisatos, *Ber. Bunsenges Phys. Chem.* **101**, 1573 (1997). One attempt to explain the absence of defects in nanocrystals is to estimate the equilibrium distance between two dislocations in the case of dislocation pileup by relating the repulsive force between two dislocations to an externally applied force (17). This model predicts that dislocations are unstable within crystallites of dimensions smaller than such a calculated distance. If we use published values for the shear modulus (18), a Burgers vector of 0.4 nm, an estimated Poisson's ratio, and hardness, the calculated minimum distance between dislocations in titania (anatase) is between 7 and 8 nm. The minimum separation is predicted to scale with the magnitude of the Burgers vector. This prediction is supported by HRTEM examination of the nanocrystalline titania used in this study, which revealed the as-synthesized particles (which are 5 to 6 nm in diameter) to be dislocation free (19).
5. Incorporation of impurities in a growing crystal and shear stress [in nanocrystalline aggregates (8)] can introduce dislocations. However, in many cases, explanations involving impurity adsorption and shear are unsatisfactory, and alternative mechanisms for dislocation formation are required.
6. R. L. Penn and J. F. Banfield, in preparation.
7. J. F. Banfield and R. J. Hamers, *Geomicrobiology: Interactions Between Microbes and Minerals*, vol. 35 of *Reviews in Mineralogy*, J. F. Banfield and K. H. Nealson, Eds. (Mineralogical Society of America, Washington, DC, 1997), pp. 86–122.
8. R. L. Penn and J. F. Banfield, *Am. Mineral.*, in press.
9. The definition of twinning was given by G. Friedel, in *étude sur les groupements cristallins*. (Bulletin de la Société de l'Industrie minière, Quatrième série, Tomes III e IV, Société de l'Imprimerie Theolier J. Thomas et C., Saint-Étienne, France, 1904).
10. T. Ito, *X-Ray Studies on Polymorphism* (Maruzen, Tokyo, Japan, 1950).
11. R. L. Penn and J. F. Banfield, in preparation.
12. A. A. Gribb and J. F. Banfield, *Am. Mineral.* **82**, 717 (1997).
13. R. S. Averback, H. Zhu, R. Tao, H. Höfler, *Synthesis and Processing of Nanocrystalline Powder*, D. L. Bourell, Ed. (The Minerals, Metals, Materials Society, Warrendale, PA, 1996).
14. Spiral growth about screw dislocations supplies a mechanism for generating a subset of the known polytypes [D. Pandey, A. Baromet, P. Krishna, *Phys. Chem. Miner.* **8**, 268 (1982); R. S. Mitchell, *Z. Kristallogr.* **109**, 1 (1957)].
15. S. Amelinckx, *C. R. Acad. Sci. Paris* **237**, 1726 (1953); W. Dekeyser, *Report of the Conference on Defects in Crystalline Solids*, July 1954, H. H. Wills Physical Laboratory, University of Bristol, Bristol, UK (The Physical Society, London, 1955). V. G. Bhide, *Zs. Krist.* **109**, 81 (1957); A. Baromet, *Prog. Crystal Growth Charact.* **1**, 151 (1978).
16. Examples include polymorphs that are long-period interstratifications of serpentine and chlorite, con-

sisting of various proportions of layer types in regularly repeating patterns [J. F. Banfield and S. W. Bailey, *Am. Mineral.* **81**, 79 (1996)].

17. G. Nieh and J. Wadsworth, *Scr. Metall. Mater.* **25**, 955 (1991); D. Sundararaman, *Mat. Sci. Eng. B Solid* **32**, 307 (1995).
18. H. J. Höfler and R. S. Averback, *Scr. Metall. Mater.* **24**, 2401 (1990).
19. A. A. Gribb, J. F. Banfield, R. L. Penn, unpublished observations.

20. We thank M. Nespolo and T. Kogure (University of Tokyo) and H. Zhang and R. J. Hamers (University of Wisconsin–Madison) for helpful discussions. Funding was provided by NSF grant EAR-9508171, a National Physical Science Consortium Scholarship to R.L.P. (sponsored by Sandia National Laboratories), and Mineralogical Society of America Grant for Student Research in Mineralogy and Petrology to R.L.P.

28 April 1998; accepted 10 July 1998

Tetravalent Uranium in Calcite

N. C. Sturchio, M. R. Antonio, L. Soderholm, S. R. Sutton, J. C. Brannon

X-ray absorption spectroscopy and x-ray fluorescence microprobe studies of 35-million-year-old calcite from a Mississippi Valley-type zinc ore deposit indicate substitution of tetravalent uranium for divalent calcium. Thus, tetravalent uranium has a stable location in calcite deposited under reducing conditions. This result validates uranium-series dating methods (including uranium/lead dating) for ancient calcite and shows that calcite provides a sink for uranium in deep groundwater aquifers and anoxic lacustrine and marine basins.

Trace amounts of U are known to occur in calcite. This occurrence is the basis for the U-series age determinations of ancient calcites (1). It is used as a marine paleoenvironmental and diagenetic indicator (2) and may influence the transport behavior of U in groundwater aquifers (3). However, the location of U in the structure of calcite is problematic. Dissolved U in most natural waters generally occurs in the hexavalent oxidation state (U⁶⁺) as the relatively large divalent uranyl ion (UO₂²⁺), which is too large for regular lattice sites in calcite (4, 5). Uranium in the tetravalent oxidation state (U⁴⁺) is generally considered to be relatively immobile because of the extremely low solubility of uranous phases (4). In addition, a direct structural measurement of U coordination in calcite at natural concentration levels (typically 0.1 to 10 μg/g) has been difficult to obtain.

To help elucidate the geochemical behavior of U in natural systems, we examined 35-million-year-old spar calcite having a relatively high U concentration [5 to 35 parts per million (ppm)] from a Mississippi Valley-type zinc ore deposit (6). We made x-ray absorption and x-ray fluorescence measurements of U in samples of this calcite and in U-rich reference materials, using synchrotron radiation (7).

The x-ray absorption near-edge structure (XANES) spectra of the sample and the U⁴⁺ reference compound have indistinguishable

peak edge energies of 20,952.4 ± 0.3 and 20,952.2 ± 0.3 eV, respectively, whereas the U⁶⁺ reference compound has a peak edge energy of 20,954.3 ± 0.3 eV (Fig. 1). These spectra indicate that U in the sample is dominantly tetravalent.

The series of sharp peaks in the radial distribution function that is obtained by Fourier transform of extended x-ray absorption fine structure (EXAFS) spectra shows that U occupies a regular and well-defined crystallographic site in the calcite sample (Fig. 2). A multishell model (Table 1) in which U substitutes for Ca in the calcite structure corresponds with the experimental data (Fig. 2). There is one important difference between the environment of Ca in calcite and the environment of U in this calcite sample. In calcite, the first coordination shell of O about Ca forms an octahedron with a Ca-O radial distance (R) of 2.36 Å (5). The O coordination about U in the calcite sample, however, is best fit with two shells: one at 2.21 Å and one at 2.78 Å. The more distant shells, including a U-C₆ shell at 3.26 Å, a U-Ca₆ shell at 4.02 Å, and a U-Ca₆ shell at 4.98 Å, have radial distances that are indistinguishable, within error, from the corresponding shells about Ca in calcite (Table 2).

The EXAFS data are well fit with one coordination environment, ruling out the presence of multiple oxidation states or defect environments. The radial distribution function shown in Fig. 2B and the coordination shell radii listed in Table 1 are inconsistent with the occurrence of U as U⁶⁺ in the uranyl ion because of the absence of the characteristic strong backscattering peak from O at about 1.8 Å. Furthermore, these data are inconsistent with the occurrence of U within inclusions of uraninite (UO₂) or coffi-

N. C. Sturchio, M. R. Antonio, L. Soderholm, Argonne National Laboratory, Argonne, IL 60439, USA. S. R. Sutton, Consortium for Advanced Radiation Sources and Department of Geophysical Sciences, University of Chicago, Chicago, IL 60637, USA. J. C. Brannon, Department of Earth and Planetary Sciences, Washington University, St. Louis, MO 63130, USA.